Quasinormal modes of charged scalars around dilaton black holes in 2 + 1 dimensions: Exact frequencies

Sharmanthie Fernando

Department of Physics & Geology, Northern Kentucky University, Highland Heights, Kentucky 41099, USA

(Received 26 February 2008; published 5 June 2008)

We have studied the charged scalar perturbation around a dilaton black hole in 2 + 1 dimensions. The wave equations of a massless charged scalar field are shown to be exactly solvable in terms of hypergeometric functions. The quasinormal frequencies are computed exactly. The relation between the quasinormal frequencies and the charge of the black hole, charge of the scalar, and the temperature of the black hole are analyzed. The asymptotic form of the real part of the quasinormal frequencies is evaluated exactly.

DOI: 10.1103/PhysRevD.77.124005 PACS numbers: 04.70.Bw

I. INTRODUCTION

When a black hole is perturbed by an external field, the dynamics of the scattered waves can be described in three stages [1]. The first corresponds to the initial wave which will depend on the source of disturbance. The second corresponds to the quasinormal modes with complex frequencies. Such modes are called quasinormal in contrast to normal modes since these are damped oscillations. The values of the quasinormal modes are independent of the initial disturbance and only depend on the parameters of the black hole. The focus of this paper is to analyze quasinormal modes of a charge scalar around a dilaton black hole in 2 + 1 dimensions. The last stage of perturbations is described by a power-law tail behavior of the corresponding field in some cases.

In recent times, there had been extensive work done to compute quasinormal modes (QNM) and to analyze them in various black hole backgrounds. A good review is Kokkotas *et al.* [2].

One of the reasons for the attention on QNM's is the conjecture relating anti-de-Sitter space (AdS) and conformal field theory (CFT) [3]. It is conjectured that the imaginary part of the QNM's which gives the time scale to decay the black hole perturbations also corresponds to the time scale of the conformal field theory (CFT) on the boundary to reach thermal equilibrium. There are many works on AdS black holes on this subject [4–7]. Also, if signals due to QNM's are detected by the gravitational wave detectors, one may be able to identify the charges of black holes and obtain deeper understanding of the inner structure of the black holes in nature. A recent review on QNM's and gravitational wave astronomy written by Ferrari and Gualtieri discusses such possibilities [8].

There are many papers on the study of perturbations of black holes by neutral scalars. However, when a charged black hole is formed with gravitational collapse of charged matter, one expects perturbations by charged fields to develop outside the black hole. Hence, it is worthwhile to study charged scalar field perturbations. The late time evolution of a charged scalar in the gravitational collapse of charged matter to form Reissner-Nordstrom black holes was analyzed by Hod and Pirani [9–11]. QNM's of a massive charged scalar field around the Reissner-Nordstrom black hole were studied by Konoplya [12]. Decay of a charged scalar and the Dirac field around the Kerr-Newmann-de-Sitter black hole were studied by Konoplya and Zhidenko in [13]. In [14], decay of massless charged scalars around a variety of black holes in four dimensions was studied by Konoplya.

To the author's knowledge, most of the works on QNM's of black holes in four and higher dimensions are numerical except for few cases. A few we are aware of are the massless topological black hole calculation done by Aros *et al.* [15], exact frequencies computed for gravitational perturbation of topological black holes in [16], and QNM computations for de Sitter space in [17,18]. However, in 2 + 1 dimensions, QNM's can be computed exactly due to the nature of the wave equations. In particular, the well-known Bañados-Teitelboim-Zanalli (BTZ) black hole [19] has been studied with exact results [20–23]. The QNM's of the neutral scalars around the dilaton black hole were computed exactly in [24]. The Dirac QNM's for the dilaton black hole were computed in [25]. In this paper we take it a step further by studying QNM's of a charged scalar around dilaton black holes in 2 + 1 dimensions which leads to exact results. To the author's knowledge, all work related to QNM's of charged scalars has been done numerically.

Extensions of the BTZ black hole with charge have led to many interesting works. The first investigation was done by Bañados *et al.* [19]. Because of the logarithmic nature of the electromagnetic potential, these solutions give rise to unphysical properties [26]. The horizonless static solution with magnetic charge was studied by Hirshmann *et al.* [27] and the persistence of these unphysical properties was highlighted by Chan [26]. Kamata *et al.* [28] presented a rotating charged black hole with self(anti-self)-duality imposed on the electromagnetic fields. The resulting solutions were asymptotic to an extreme BTZ black hole

solution but had diverging mass and angular momentum [26]. Clement [29], Fernando and Mansouri [30] introduced a Chern-Simons term as a regulator to screen the electromagnetic potential and obtained horizonless charged particlelike solutions. In this paper we consider an interesting class of black hole solutions obtained by Chan and Mann [31]. The solutions represent static charged black holes with a dilaton field. It is a solution to low-energy string action. Furthermore, it has finite mass unlike some of the charged black holes described above.

We have organized the paper as follows: In Sec. II an introduction to the geometry of the black hole is given. The charge scalar perturbation of the black hole is given in Sec. III. The general solution to the wave equation is given in Sec. IV. A solution with boundary conditions is given in Sec. V. QNM frequencies of the black hole are computed and analyzed in detail in Sec. VI. Finally the conclusion is given in Sec. VII.

II. GEOMETRY OF THE STATIC CHARGED DILATON BLACK HOLE

In this section we will present the geometry and important details of the static charged black hole. The Einstein-Maxwell-dilaton action which led to these black holes considered by Chan and Mann [31] is given as follows:

$$S = \int d^3x\sqrt{-g}[R - 4(\nabla\phi)^2 - e^{-4\phi}F_{\mu\nu}F^{\mu\nu} + 2e^{4\phi}\Lambda]. \tag{1}$$

Here, Λ is treated as the cosmological constant. In [31], it was discussed that black hole solutions exist only for $\Lambda > 0$. Hence throughout this paper we will treat $\Lambda > 0$. The parameter ϕ is the dilaton field, R is the scalar curvature, and $F_{\mu\nu}$ is the Maxwell's field strength in the action. This action is conformally related to the low-energy string action in $2 + 1$ dimensions. The static circularly symmetric solution to the above action is given by

$$\begin{aligned} ds^2 &= -f(r)dt^2 + \frac{4r^2dr^2}{f(r)} + r^2d\theta^2 \\ f(r) &= (-2Mr + 8\Lambda r^2 + 8Q^2); \\ \phi &= \frac{1}{4}\ln\left(\frac{r}{\beta}\right); \qquad F_{rt} = \frac{Q}{r^2}. \end{aligned} \tag{2}$$

For $M \geq 8Q\sqrt{\Lambda}$, the space-time represents a black hole. It has two horizons given by the zeros of g_{tt};

$$\begin{aligned} r_+ &= \frac{M + \sqrt{M^2 - 64Q^2\Lambda}}{8\Lambda}; \\ r_- &= \frac{M - \sqrt{M^2 - 64Q^2\Lambda}}{8\Lambda}. \end{aligned} \tag{3}$$

There is a singularity at $r = 0$ and it is timelike. Note that in the presence of a nontrivial dilaton, the space geometry of the black hole does not behave as either de Sitter ($\Lambda < 0$) or anti-de-Sitter ($\Lambda > 0$) [31]. An important thermodynamical quantity corresponding to a black hole is the Hawking temperature T_H. It is given by

$$T_H = \frac{1}{4\pi}\left|\frac{dg_{tt}}{dr}\left|\sqrt{-g^{tt}g^{rr}}\right|\right|_{r=r_+} = \frac{M}{4\pi r_+}\sqrt{1 - \frac{64Q^2\Lambda}{M^2}}. \tag{4}$$

The temperature $T_H = 0$ for the extreme black hole with $M = 8Q\sqrt{\Lambda}$. For the uncharged black hole $T_H = \frac{\Lambda}{\pi}$. This black hole is also a solution to low-energy string action by a conformal transformation,

$$g^{\text{string}} = e^{4\phi}g^{\text{Einstein}}. \tag{5}$$

In string theory, it is possible to create charged solutions from uncharged ones by duality transformations. For a review of such transformations see Horowitz [32]. It is possible to apply such transformations to the uncharged black hole with charge $Q = 0$ in the metric in Eq. (2) to obtain the charged black hole with $Q \neq 0$. Such a duality was discussed in detail in the paper by Fernando [24].

III. CHARGED SCALAR PERTURBATION OF DILTON BLACK HOLES

We will develop the equations for a charged scalar field in the background of the static charged dilaton black hole in this section. The general equation for a massless charged scalar field in curved space-time can be written as

$$\nabla^\mu\nabla_\mu\Phi + (ie)^2A^\mu A_\mu\Phi - 2ieA^\mu\partial_\mu\Phi - ie\Phi\nabla^\mu A_\mu = 0. \tag{6}$$

Using the anzatz,

$$\Phi = e^{im\theta}\frac{\eta(t, r)}{\sqrt{r}}, \tag{7}$$

Eq. (6) simplifies to

$$\frac{\partial^2\eta(t, r)}{\partial t^2} - \frac{\partial^2\eta(t, r)}{\partial r_*^2} + \frac{2ieQ}{r}\frac{\partial\eta(t, r)}{\partial t} + V(r)\eta(t, r) = 0. \tag{8}$$

Here, $V(r)$ is given by

$$V(r) = \frac{f(r)}{2r^{3/2}}\frac{d}{dr}\left(\frac{f(r)}{4r^{3/2}}\right) + \frac{m^2f(r)}{r^2} - \frac{e^2Q^2}{r^2} \tag{9}$$

and r_* is the tortoise coordinate computed as

$$\begin{aligned} dr_* &= \frac{2rdr}{f(r)} \Rightarrow r_* \\ &= \frac{1}{4\Lambda(r_+ - r_-)}(r_+\ln(r - r_+) - r_-\ln(r - r_-)). \end{aligned} \tag{10}$$

Note that when $r \to r_+$, $r_* \to -\infty$ and for $r \to \infty$, $r_* \to \infty$. The function $f(r)$ is given by Eq. (2) in Sec. II. By

substituting the function $f(r)$ into Eq. (9), one can obtain a simplified version of the potential $V(r)$ as

$$V(r) = -\frac{12Q^4}{r^4} + \frac{4MQ^2}{r^3} + \frac{1}{r^2}\left(-\frac{M^2}{4} + 8m^2Q^2 - 8Q^2\Lambda - e^2Q^2\right) - \frac{2m^2M}{r} + (8m^2\Lambda + 4\Lambda^2). \tag{11}$$

Note that if the function $\eta(t, r)$ is redefined as

$$\eta(t, r) = e^{-i\omega t}\xi(r_*), \tag{12}$$

the wave equation will simplifies to the equation,

$$\left(\frac{d^2}{dr_*^2} + \omega^2 + \frac{2eQ\omega}{r} - V(r)\right)\xi(r_*) = 0. \tag{13}$$

It is clear that if $e = 0$, Eq. (13) becomes the *Schrödinger*-type equation with a potential $V_{e=0}(r)$ given by

$$V_{e=0}(r) = -\frac{12Q^4}{r^4} + \frac{4MQ^2}{r^3} + \frac{1}{r^2}\left(-\frac{M^2}{4} + 8m^2Q^2 - 8Q^2\Lambda\right) - \frac{2m^2M}{r} + (8m^2\Lambda + 4\Lambda^2). \tag{14}$$

The potentials are plotted in Fig. 1. The greater the value e of the charged scalar, the smaller the peak of the potential.

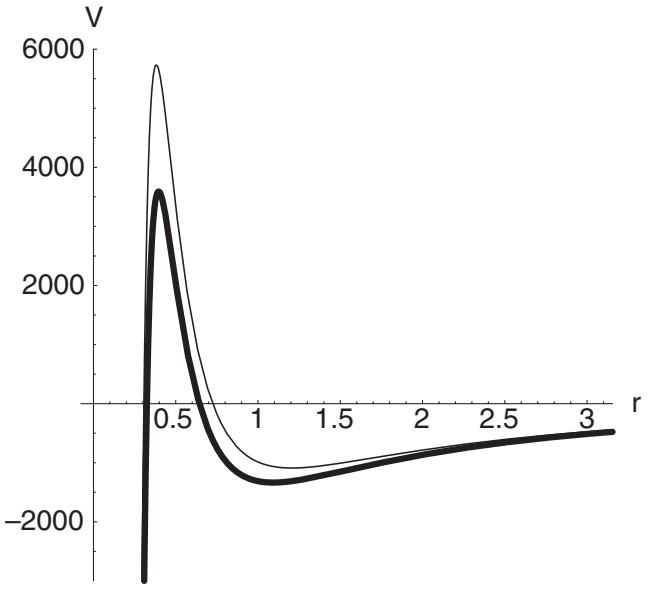

FIG. 1. The behavior of the potentials $V(r)$ and $V_{e=0}(r)$ with r for $\Lambda = 2$ $M = 120$, $Q = 3$, $m = 2$, and $e = 6$. The dark curve represents $V(r)$ and the light curve represents $V_{e=0}(r)$.

IV. GENERAL SOLUTION TO THE CHARGED SCALAR WAVE EQUATION

In order to find exact solutions to the wave equation for the charged scalar, we will revisit Eq. (6) in Sec. III. Using the anzatz,

$$\Phi = e^{-i\omega t}e^{im\theta}R(r), \tag{15}$$

Eq. (6) leads to the radial equation,

$$\frac{d}{dr}\left(\frac{f(r)}{2}\frac{dR(r)}{dr}\right) + 2r^2\left(\frac{\omega^2}{f(r)} - \frac{m^2}{r^2}\right)R(r) - \frac{4eQ\omega rR(r)}{f(r)} + \frac{2e^2Q^2R(r)}{f(r)} = 0. \tag{16}$$

In order to solve the wave equation exactly, one can redefine the r coordinate of Eq. (16) with a new variable z given by

$$z = \left(\frac{r - r_+}{r - r_-}\right). \tag{17}$$

Note that in the new coordinate system, $z = 0$ corresponds to the horizon r_+ and $z = 1$ corresponds to infinity. With the new coordinate, Eq. (16) becomes

$$z(1 - z)\frac{d^2R}{dz^2} + (1 - z)\frac{dR}{dz} + P(z)R = 0. \tag{18}$$

Here,

$$P(z) = \frac{A}{z} + \frac{B}{-1 + z} + C, \tag{19}$$

where

$$A = \frac{(r_+\omega - eQ)^2}{16(r_+ - r_-)^2\Lambda^2}; \qquad B = \frac{8m^2\Lambda - \omega^2}{16\Lambda^2}; \qquad C = -\frac{(r_-\omega - eQ)^2}{16(r_+ - r_-)^2\Lambda^2}. \tag{20}$$

Now, if $R(z)$ is redefined as

$$R(z) = z^\alpha(1 - z)^\beta F(z), \tag{21}$$

the radial equation given in Eq. (18) becomes

$$z(1 - z)\frac{d^2F}{dz^2} + (1 + 2\alpha - (1 + 2\alpha + 2\beta)z)\frac{dF}{dz} + \left(\frac{\bar{A}}{z} + \frac{\bar{B}}{-1 + z} + \bar{C}\right)F = 0, \tag{22}$$

where

$$\bar{A} = A + \alpha^2 \qquad \bar{B} = B + \beta - \beta^2 \qquad \bar{C} = C - (\alpha + \beta)^2. \tag{23}$$

The above equation resembles the hypergeometric differential equation which is of the form [33]

$$z(1-z)\frac{d^2F}{dz^2} + (c-(1+a+b)z)\frac{dF}{dz} - abF = 0. \quad (24)$$

By comparing the coefficients of Eq. (22) and (24), one can obtain the following identities:

$$c = 1 + 2\alpha \quad (25)$$

$$a + b = 2\alpha + 2\beta \quad (26)$$

$$\bar{A} = A + \alpha^2 = 0; \Rightarrow \alpha = \pm\frac{i(r_+\omega - eQ)}{4\Lambda(r_+ - r_-)} \quad (27)$$

$$\bar{B} = B + \beta - \beta^2 = 0; \Rightarrow \beta = \frac{1 + i\sqrt{(\frac{\omega^2 - 8m^2\Lambda}{4\Lambda} - 1)}}{2} \quad (28)$$

$$ab = -\bar{C} = (\alpha+\beta)^2 - C. \quad (29)$$

From Eqs. (26) and (29),

$$a = \alpha + \beta + \gamma \qquad b = \alpha + \beta - \gamma. \quad (30)$$

Here,

$$\gamma = \sqrt{C} = \pm\frac{i(r_-\omega - eQ)}{4\Lambda(r_+ - r_-)}. \quad (31)$$

With the above values for a, b, and c, the solution to the hypergeometric function $F(z)$ is given by [33]

$$F(a,b,c;z) = \frac{\Gamma(c)}{\Gamma(a)\Gamma(b)}\Sigma\frac{\Gamma(a+n)\Gamma(b+n)}{\Gamma(c+n)}\frac{z^n}{n!} \quad (32)$$

with a radius of convergence being the unit circle $|z| = 1$. Hence the general solution to the radial part of the charged scalar wave equation is given by

$$R(z) = z^\alpha(1-z)^\beta F(a,b,c;z) \quad (33)$$

with a, b, and c given in the above equations. The general solution for the charged wave scalar equation is

$$\Phi(z,t,\theta) = z^\alpha(1-z)^\beta F(a,b,c;z)e^{im\theta}e^{-i\omega t}. \quad (34)$$

V. SOLUTION WITH BOUNDARY CONDITIONS

In this section we will obtain solutions to the charged scalar with the boundary condition that the wave is purely ingoing at the horizon. The solutions are analyzed closer to the horizon and at infinity to obtain exact results for the wave function.

A. Solution at the near-horizon region

First, the solution of the wave equation closer to the horizon is analyzed. For the charged black hole,

$$z = \frac{(r-r_+)}{(r-r_-)} \quad (35)$$

and as the radial coordinate r approaches the horizon, z approaches 0. In the neighborhood of $z = 0$, the hypergeometric function has two linearly independent solutions given by [33]

$$F(a,b;c;z) \quad \text{and} \quad z^{(1-c)}F(a-c+1, b-c+1; 2-c; z). \quad (36)$$

Substituting the values of a, b, c in terms of α, β, and γ, the general solution for $R(z)$ can be written as

$$R(z) = C_1 z^\alpha(1-z)^\beta F(\alpha+\beta+\gamma, \alpha+\beta-\gamma, 1+2\alpha, z) + C_2 z^{-\alpha}(1-z)^\beta F(-\alpha+\beta+\gamma, -\alpha+\beta-\gamma, 1-2\alpha, z). \quad (37)$$

Here, C_1 and C_2 are constants to be determined. Before proceeding any further, we want to point out that the above equation is symmetric for $\alpha \leftrightarrow -\alpha$. Note that in Eq. (27), α could have both $\pm$ signs. Because of the above symmetry in Eq. (37), we will choose the " +" sign for α for the rest of the paper.

Since closer to the horizon $z \to 0$, the above solution in Eq. (37) approaches

$$R(z \to 0) = C_1 z^\alpha + C_2 z^{-\alpha}. \quad (38)$$

Closer to the horizon, $r \to r_+$. Hence, z can be approximated with

$$z \approx \frac{r - r_+}{r_+ - r_-}. \quad (39)$$

The "tortoise" coordinate for the charged black hole is given in Eq. (10). Near the horizon $r \to r_+$, the tortoise coordinate can be approximated to be

$$r_* \approx \frac{r_+}{4\Lambda(r_+ - r_-)}\ln(r - r_+). \quad (40)$$

Hence,

$$r - r_+ = e^{(4\Lambda(r_+ - r_-)/r_+)r_*} \quad (41)$$

leading to

$$z \approx \frac{r - r_+}{r_+ - r_-} = \frac{1}{(r_+ - r_-)}e^{(4\Lambda(r_+ - r_-)/r_+)r_*}. \quad (42)$$

Hence Eq. (38) can be rewritten in terms of r_* as

$$R(r \to r_+) = C_1\left(\frac{1}{r_+ - r_-}\right)^\alpha e^{i\hat{\omega}r_*} + C_2\left(\frac{1}{r_+ - r_-}\right)^{-\alpha} e^{-i\hat{\omega}r_*}. \quad (43)$$

To obtain the above expression, α is substituted from Eq. (27) and

$$\hat{\omega} = \omega - \frac{eQ}{r_+}. \quad (44)$$

The first and the second term in Eq. (43) corresponds to the

outgoing and the ingoing wave, respectively. Now, one can impose the condition that the wave is purely ingoing at the horizon. Hence we pick $C_1 = 0$ and $C_2 \neq 0$. Therefore the solution closer to the horizon is

$$R(z \to 0) = C_2 z^{-\alpha}(1-z)^{\beta} F(-\alpha+\beta+\gamma, -\alpha+\beta-\gamma, 1-2\alpha, z). \tag{45}$$

B. Solution at asymptotic region

Now the question is what the wave equation is when $r \to \infty$. For large r, the function $f(r) \to 8\Lambda r^2$. When $f(r)$ is replaced with this approximated function in the wave equation given by Eq. (16), it simplifies to

$$\frac{d}{dr}\left(4\Lambda r^2 \frac{dR(r)}{dr}\right) + 2r^2\left(\frac{\omega^2}{8\Lambda r^2} - \frac{m^2}{r^2}\right)R(r) - \frac{eQ\omega R(r)}{2\Lambda r} + \frac{e^2Q^2R(r)}{4\Lambda r^2} = 0. \tag{46}$$

For large r, one can neglect the last two terms in the above equation. Hence finally, the wave equation at large r can be expanded to be

$$r^2R'' + 2rR' + pR = 0, \tag{47}$$

where

$$p = \frac{\omega^2}{16\Lambda^2} - \frac{m^2}{2\Lambda}. \tag{48}$$

One can observe that $p = -B$ from Eq. (20). Also Eq. (47) is the well-known Euler equation with the solution

$$R(r) = D_1\left(\frac{r_+ - r_-}{r}\right)^{a_1} + D_2\left(\frac{r_+ - r_-}{r}\right)^{a_2} \tag{49}$$

with

$$a_1 = \frac{1+\sqrt{1-4p}}{2} = \beta; \qquad a_2 = \frac{1-\sqrt{1-4p}}{2} = (1-\beta). \tag{50}$$

The expression for β is given in Eq. (28). Note that the form in Eq. (49) is chosen to facilitate to compare it with the matching solutions in Sec. V C.

C. Matching the solutions at the near horizon and the asymptotic region

In this section we match the asymptotic solution given in Eq. (49) to the large r limit (or the $z \to 1$) of the near-horizon solution given in Eq. (45) to obtain an exact expression for D_1 and D_2. To obtain the $z \to 1$ behavior of Eq. (45), one can perform a well-known transformation on hypergeometric function given as follows [33]:

$$F(a,b,c,z) = \frac{\Gamma(c)\Gamma(c-a-b)}{\Gamma(c-a)\Gamma(c-b)}F(a,b;a+b-c+1;1-z) + (1-z)^{c-a-b}\frac{\Gamma(c)\Gamma(a+b-c)}{\Gamma(a)\Gamma(b)} \times F(c-a,c-b;c-a-b+1;1-z). \tag{51}$$

Applying this transformation to Eq. (45) and substituting for the values of a, b, and c, one can obtain the solution to the wave equation in the asymptotic region as follows:

$$\begin{aligned} R(z) = {} & C_2 z^{-\alpha}(1-z)^{\beta} \\ & \times \frac{\Gamma(1-2\alpha)\Gamma(1-2\beta)}{\Gamma(1-\alpha-\beta-\gamma)\Gamma(1-\alpha-\beta+\gamma)} \\ & \times F(-\alpha+\beta+\gamma, -\alpha+\beta-\gamma; 2\beta; 1-z) \\ & + C_2 z^{-\alpha}(1-z)^{1-\beta} \\ & \times \frac{\Gamma(1-2\alpha)\Gamma(-1+2\beta)}{\Gamma(-\alpha+\beta+\gamma)\Gamma(-\alpha+\beta-\gamma)} \\ & \times F(1-\alpha-\beta-\gamma, 1-\alpha-\beta \\ & + \gamma; 2-2\beta; 1-z). \end{aligned} \tag{52}$$

Now we can take the limit of $R(z)$ as $z \to 1$ (or $r \to \infty$) which will lead to

$$\begin{aligned} R(z \to 1) = {} & C_2(1-z)^{\beta}\frac{\Gamma(1-2\alpha)\Gamma(1-2\beta)}{\Gamma(1-\alpha-\beta-\gamma)\Gamma(1-\alpha-\beta+\gamma)} \\ & + C_2(1-z)^{1-\beta}\frac{\Gamma(1-2\alpha)\Gamma(-1+2\beta)}{\Gamma(-\alpha+\beta+\gamma)\Gamma(-\alpha+\beta-\gamma)}. \end{aligned} \tag{53}$$

Note that we have replaced $F(a, b, c, 1-z)$ and z^{α} with 1 when z approaches 1. Since

$$1 - z = \frac{r_+ - r_-}{r - r_-}, \tag{54}$$

for large r, the above can be approximated with

$$1 - z \approx \frac{r_+ - r_-}{r}. \tag{55}$$

By replacing $1 - z$ with the above expression in Eq. (55), $R(r)$ for large r can be written as

$$\begin{aligned} R(r \to \infty) = {} & C_2\left(\frac{r_+ - r_-}{r}\right)^{\beta} \\ & \times \frac{\Gamma(1-2\alpha)\Gamma(1-2\beta)}{\Gamma(1-\alpha-\beta-\gamma)\Gamma(1-\alpha-\beta+\gamma} \\ & + C_2\left(\frac{r_+ - r_-}{r}\right)^{1-\beta} \\ & \times \frac{\Gamma(1-2\alpha)\Gamma(-1+2\beta)}{\Gamma(-\alpha+\beta+\gamma)\Gamma(-\alpha+\beta-\gamma)}. \end{aligned} \tag{56}$$

By comparing Eqs. (49) and (56), the coefficients D_1 and

D_2 can be written as

$$D_1 = C_2 \frac{\Gamma(1-2\alpha)\Gamma(1-2\beta)}{\Gamma(1-\alpha-\beta+\gamma)\Gamma(1-\alpha-\beta-\gamma)} \quad (57)$$

$$D_2 = C_2 \frac{\Gamma(1-2\alpha)\Gamma(-1+2\beta)}{\Gamma(-\alpha+\beta+\gamma)\Gamma(-\alpha+\beta-\gamma)}. \quad (58)$$

To determine which part of the solution in Eq. (49) corresponds to the ''ingoing'' and ''outgoing'' respectively, we will first find the tortoise coordinate r_* in terms of r at large r. Note that for large r, $f(r) \to 8\Lambda r^2$. Hence the equation relating the tortoise coordinate r_* and r in Eq. (10) simplifies to

$$dr_* = \frac{dr}{4\Lambda r}. \quad (59)$$

The above can be integrated to obtain

$$r_* \approx \frac{1}{4\Lambda} \ln\left(\frac{r}{r_+}\right). \quad (60)$$

Hence,

$$r \approx r_+ e^{4\Lambda r_*}. \quad (61)$$

Substituting r from Eq. (61) and β from Eq. (28) into Eq. (49), $R(r \to \infty)$ is rewritten as

$$\begin{aligned} R(r\to\infty) \to\ & D_1\left(\frac{r_+ - r_-}{r_+}\right)^{\beta} \\ & \times e^{-i\omega r_* \sqrt{1-(4\Lambda^2/\omega^2)((2m^2/\Lambda)+1)} - 2\Lambda r_*} \\ & + D_2\left(\frac{r_+ - r_-}{r_+}\right)^{1-\beta} \\ & \times e^{i\omega r_* \sqrt{1-(4\Lambda^2/\omega^2)((2m^2/\Lambda)+1)} - 2\Lambda r_*}. \end{aligned} \quad (62)$$

From the above it is clear that the first term and the second term represent the ingoing and outgoing waves, respectively.

VI. QUASINORMAL MODES OF THE DILATON BLACK HOLE

Quasinormal modes of a classical perturbation of black hole space-times are defined as the solutions to the related wave equations with purely ingoing waves at the horizon. In addition, one has to impose boundary conditions on the solutions at the asymptotic region as well. In asymptotically flat space-times, the second boundary condition is the solution to be purely outgoing at spatial infinity. For non-asymptotically flat space-times, there are two possible boundary conditions to impose at sufficiently large distances from the black hole horizon: one is the field to vanish at large distances and the other is for the flux of the field to vanish at far from the horizon. Here, we will choose the first. This is the condition imposed in Ref. [24]. Another example in $2+1$ dimensions, where the vanishing of the field at large distance is imposed, is given in Ref. [20] where QNM's of scalar perturbations of BTZ black holes were computed exactly.

Let us consider the field $R(r)$ at large distances given by Eq. (56). Clearly the second term vanishes when $r \to \infty$. This also can be seen from Eq. (52) where the second term vanishes for $z \to 1$. Since C_2 is not zero, the first term vanishes only at the poles of the Gamma functions $\Gamma(1-\alpha-\beta+\gamma)$ or $\Gamma(1-\alpha-\beta-\gamma)$. Note that the Gamma function $\Gamma(x)$ has poles at $x = -n$ for $n = 0, 1, 2\ldots$. Hence to obtain QNM's, the following relation has to hold:

$$1-\alpha-\beta-\gamma = -n \quad (63)$$

or

$$1-\alpha-\beta+\gamma = -n. \quad (64)$$

The above two equations lead to two possibilities for β as follows:

$$\beta = (1+n) - \alpha \pm \gamma. \quad (65)$$

We want to recall here that γ in Eq. (31) could have both signs. Because of the nature of Eq. (65), there is no need to choose a specific sign to proceed from here. The two possibilities lead to two equations for β given by

$$\beta = (1+n) - \frac{i\omega}{4\Lambda} \quad (66)$$

and

$$\beta = (1+n) - i(\kappa_1\omega - \kappa_2 eQ), \quad (67)$$

where

$$\kappa_1 = \frac{1}{4\Lambda}\left(\frac{r_+ + r_-}{r_+ - r_-}\right); \qquad \kappa_2 = \frac{1}{2\Lambda(r_+ - r_-)}. \quad (68)$$

By combining the above equations with Eq. (28) given by

$$\frac{m^2}{2\Lambda} - \frac{\omega^2}{16\Lambda^2} = -\beta + \beta^2, \quad (69)$$

one can obtain the quadratic equation for ω given by

$$\begin{aligned} & \omega^2\left(\frac{1}{(16\Lambda^2\kappa_1^2 - 1)}\right) + \omega(i(2n+1)\kappa_1 - 2\kappa_1\kappa_2 eQ) \\ & \quad + \left(\frac{m^2}{2\Lambda} - n^2 - n - i(2n+1)\kappa_1 eQ + (\kappa_2 eQ)^2\right). \end{aligned} \quad (70)$$

Note that the β in Eq. (66) corresponds to the QNM's of the neutral scalars for the uncharged black hole with $Q = 0$ leading to $r_- = 0$. Hence by taking $r_- = 0$ in κ_1, one recovers the quadratic equation for the neutral scalar for $Q = 0$. One can solve the above quadratic equation to obtain exact values of QNM frequencies ω. There are three cases one can consider: QNM's of neutral scalars (for $Q = 0$ and $Q \neq 0$) and charged scalars. The QNM's of the neutral scalars were analyzed in detail in the paper by

Fernando [24]. We will anyway state the results in order to compare the QNM's of the charged scalars in the following section.

A. QNM frequencies of neutral scalars with $e = 0$

By letting $e = 0$ in the quadratic equation given above, one can solve it for ω as discussed in [24]. First, one can consider the QNM's for the uncharged black hole with $Q = 0$. The solution for ω is given as

$$\omega = \frac{-2i}{2n+1}(2\Lambda n(1+n) - m^2). \tag{71}$$

They are pure imaginary. Because of the minus sign in front, these oscillations will be damped leading to stable perturbations for $2\Lambda n(1+n) > m^2$. However, for $2\Lambda n(1+n) < m^2$, the oscillations would lead to unstable modes. This was pointed out in [25].

One can also compute the QNM's for the neutral scalar for the charged dilaton black hole with $Q \neq 0$ as

$$\omega = \frac{-i}{(16\Lambda^2\kappa_1^2 - 1)}(8\Lambda^2\kappa_1(1+2n) + 2\sqrt{2m^2\Lambda(16\Lambda^2\kappa_1^2 - 1) + 4\Lambda^2(4\Lambda^2\kappa_1^2 + n^2 + n)}). \tag{72}$$

Note that $16\Lambda^2\kappa_1 > 1$ and ω will always be pure imaginary. Also, due to the minus sign in front, these oscillations will be damped leading to stable neutral scalar perturbations.

B. QNM's of the charged scalar with $e \neq 0$

Now, one can solve Eq. (70) to obtain the exact results for the QNM frequencies for the charged scalar as

$$\omega = \frac{1}{(16\Lambda^2\kappa_1^2 - 1)}(-i8\Lambda^2\kappa_1(1+2n) + 16e\kappa_1\kappa_2 Q\Lambda^2 - 2i\sqrt{2m^2\Lambda(16\Lambda^2\kappa_1^2 - 1) + 4\Lambda^2(4\Lambda^2\kappa_1^2 + n^2 + n) - 4e^2\kappa_2^2 Q^2\Lambda^2 + 4ie\kappa_2 Q\Lambda^2(2n+1)}). \tag{73}$$

ω is not pure imaginary in this case: it has a real part which depends on e. For $e \to 0$, the above QNM approaches the values for the neutral scalar in Eq. (72). To separate the real part and the imaginary part of ω, the part inside the square root is redefined as follows: Let the parameters z_1, z_2, ρ, and Z be defined as

$$z_1 = 2m^2\Lambda(16\Lambda^2\kappa_1^2 - 1) + 4\Lambda^2(4\Lambda^2\kappa_1^2 + n^2 + n) - 4e^2\kappa_2^2 Q^2\Lambda^2 \tag{74}$$

$$z_2 = 4e\kappa_2 Q\Lambda^2(2n+1) \tag{75}$$

$$Z = \sqrt{z_1^2 + z_2^2} \tag{76}$$

$$\rho = \tan^{-1}\left(\frac{z_2}{z_1}\right). \tag{77}$$

Then, $\omega = \omega_{\text{real}} + i\omega_{\text{imaginary}}$ can be separated with

$$\omega_{\text{real}} = \frac{1}{(16\Lambda^2\kappa_1^2 - 1)}(16e\kappa_1\kappa_2 Q\Lambda^2 + 2\sqrt{Z}\sin(\rho/2)) \tag{78}$$

$$\omega_{\text{imaginary}} = \frac{1}{(16\Lambda^2\kappa_1^2 - 1)}(-8\Lambda^2\kappa_1(1+2n) - 2\sqrt{Z}\cos(\rho/2)). \tag{79}$$

When $e \to 0$, $\rho \to 0$ which leads to $\omega_{\text{real}} \to 0$ as expected.

In Fig. 2, $\omega_{\text{imaginary}}$ is plotted against the charge Q of the black hole. It is clear that the magnitude of $\omega_{\text{imaginary}}$ is larger for the charged scalar in comparison to the neutral scalar. Hence, the neutral scalar decays slower compared to the charged scalar. A similar behavior was observed in the charged scalar decay compared to the neutral scalar in Reissner-Nordstrom and Reissner-Nordstrom anti-de-Sitter black hole [14].

Next, we observe the behavior of ω vs charge e for two different values of black hole charge Q as given in Fig. 3.

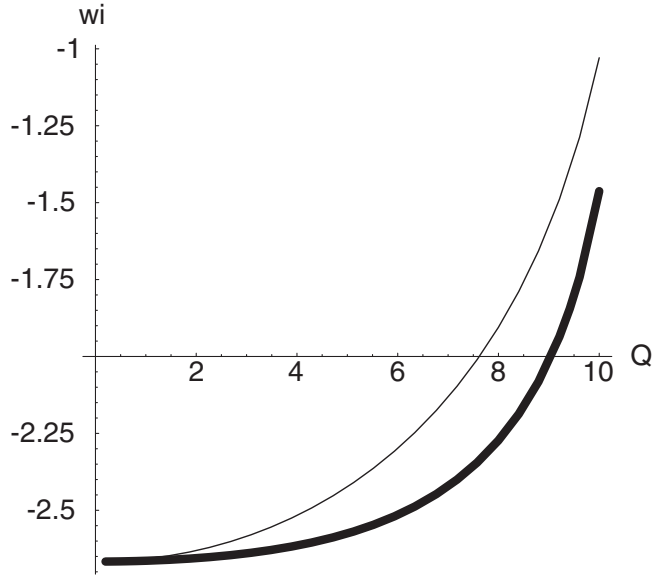

FIG. 2. The imaginary part of ω vs Q for $\Lambda = 2$ $M = 120$, $m = 2$, and $n = 1$. The dark curve represents the curve for $e = 4$ and the light curve represents for $e = 0$.

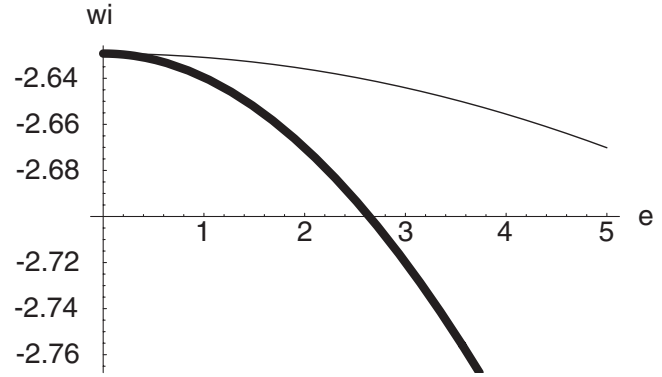

FIG. 3. The imaginary part of ω vs e for $\Lambda = 2$ $M = 120$, $m = 2$, and $n = 1$. The dark curve represents the curve for $Q = 5$ and the light curve represents for $Q = 2$.

The higher the Q, the larger the $\omega_{\text{imaginary}}$. Similarly, the real part of ω is larger for large Q as given in Fig. 4.

In Fig. 5, $\omega_{\text{imaginary}}$ is plotted vs the temperature of the black hole. For both the neutral scalar and the charged scalar, there is a linear behavior of $\omega_{\text{imaginary}}$ vs T.

In Fig. 6, the behavior of $\omega_{\text{imaginary}}$ is plotted vs the horizon radius r_+. It is concluded that, for the same r_+, the neutral scalar has a smaller decay rate than the charged scalar.

As noted in the Introduction, there are several papers focused on computing the asymptotic value of the ω_{real} of black holes with regard to the quantization of the black holes. In Fig. 7, ω_{real} is plotted vs n. It is observed that it reaches a constant for large n. The asymptotic from of the

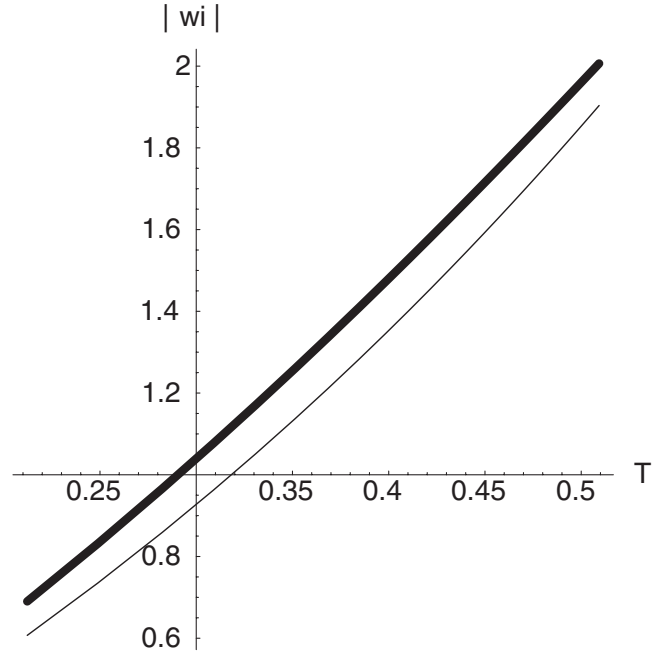

FIG. 5. The imaginary part of ω vs T for $\Lambda = 2$ $r_- = 2$, $m = 2$, and $n = 1$. The dark curve represents the curve for fixed $e = 2$ and the light curve represents for fixed $e = 0$.

real part of QNM is computed taking the limit of ω_{real} as $n \to \infty$: the value is simply

$$\omega_{\text{real}}(n \to \infty) = \frac{e\sqrt{r_p \Lambda}}{\sqrt{r_m}}. \tag{80}$$

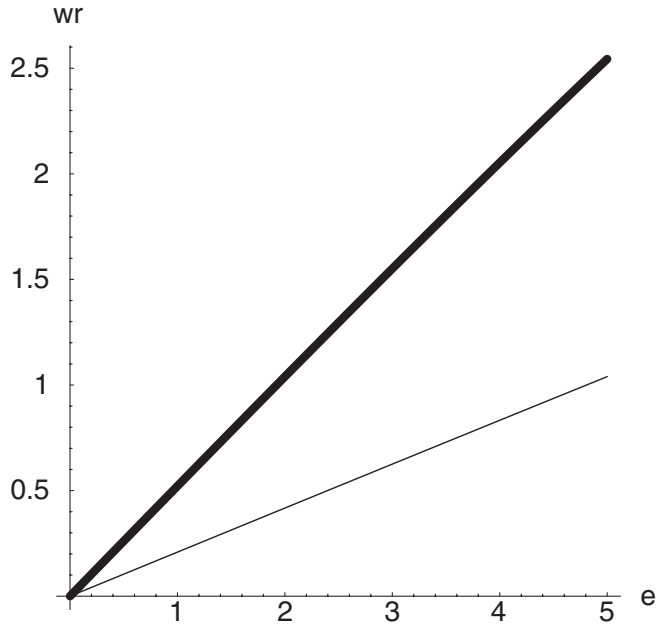

FIG. 4. The real part of ω vs e for $\Lambda = 2$ $M = 120$, $m = 2$, and $n = 1$. The dark curve represents the curve for $Q = 5$ and the light curve represents for $Q = 2$.

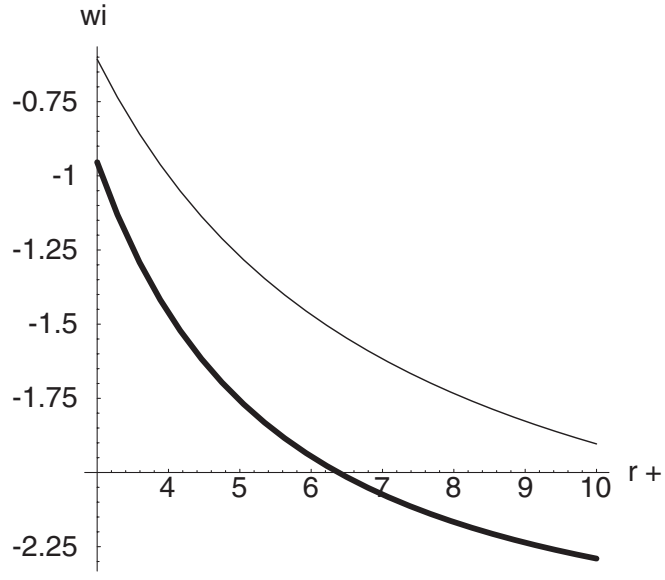

FIG. 6. The imaginary part of ω vs r_+ for $\Lambda = 2$ $r_m = 2$, $m = 2$, and $n = 1$. The dark curve represents the curve for $e = 4$ and the light curve represents for fixed $e = 0$.

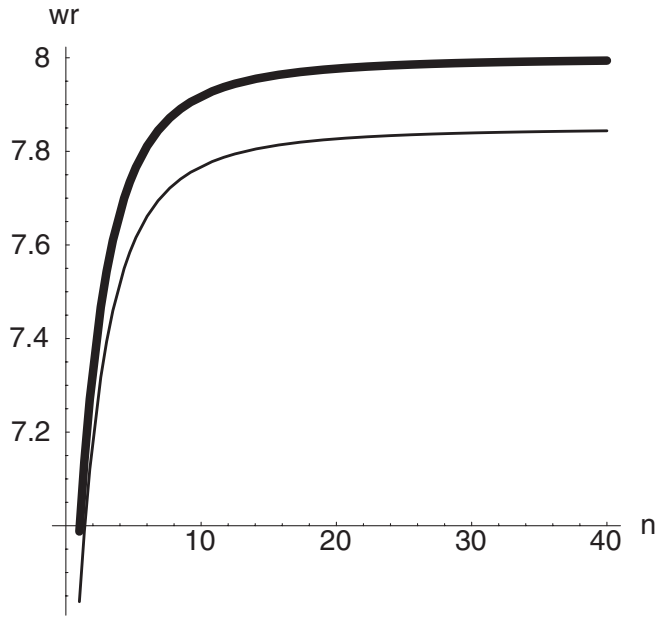

FIG. 7. The real part of ω vs n for $\Lambda = 2$, $r_p = 4$, $r_m = 2$, and $m = 2$. The dark curve represents the curve for $e = 4$ and the light curve represents for fixed $e = 3.9$.

VII. CONCLUSION

We have studied the perturbation of the dilaton black hole in $2 + 1$ by a charged scalar. The wave equations are solved exactly as hypergeometric functions. The QNM frequencies are computed exactly. It is observed that the QNM's have both a real and an imaginary component. The QNM's of the neutral scalars were pure imaginary [24]. Also it is noted that the charged scalars decay faster compared to the neutral scalars for a given black hole. This observation is in agreement with the behavior observed by Konoplya [14] in Reissner-Nordstrom and Reissner-Nordstrom-anti-de-Sitter black holes in four dimensions. The behavior of ω with various parameters are analyzed in detail. We observe the linear relation of $\omega_{\text{imaginary}}$ with the temperature of the black hole. Similar observations were reported for QNM frequencies of higher dimensions in AdS space in [4]. The asymptotic value of ω_{real} is computed to be $\frac{e\sqrt{r_p\Lambda}}{\sqrt{r_m}}$.

It would be interesting to compute the greybody factors and particle emission rates for the charged scalars for this black hole. The greybody factors were studied for the neutral scalar in [34]. Since the wave equation has been already solved, it should be a welcome step towards understanding the Hawking radiation from these black holes. There are few works related to such computations of charged particles: the particle emission by charged leptons from nonrotating black holes by Page [35] and emission of charged particles by four- and five-dimensional black holes by Gubser and Klebanov [36].

Since the asymptotic values of the real part of the QNM frequencies are computed exactly, it would be interesting to study the area spectrum of these black holes along the lines of the work by Setare [37,38].

Another interesting avenue to proceed would be to analyze the QNM's of the extreme dilaton black hole studied in this paper. Some extreme black holes have proven to be supersymmetric. For example, the extreme Reissner-Nordstrom black hole is shown to be supersymmetric since it can be embedded in $N = 2$ supergravity theory [39]. Onozawa *et al.* [40] showed that the QNM's of the extreme Reissner-Nordstrom black hole for spin $1, 3/2$, and 2 are the same. If it is possible to find a suitable supergravity theory to embed the dilaton black hole in this paper, one may be able to observe if extremality plays a role in it. Hence it would be interesting to compute the QNM's for the extreme dilaton black hole in $2 + 1$ dimensions for the charged Dirac fields and vector fields along with the charged scalar to understand such behavior in low dimensions.

The dilaton black hole considered in this paper is one of the most favorable charged black holes in $2 + 1$ dimensions to study many issues discussed above in a simpler setting with exact values for QNM frequencies.

[1] V. P. Frolov and I. D. Novikov, *Black Hole Physics: Basic Concepts and New Developments* (Kluwer Academic Publishers, Dordrecht, 1998).
[2] K. D. Kokkotas and B. G. Schmidt, Living Rev. Relativity **2**, 2 (1999), http://www.livingreviews.org.
[3] O. Aharony, S. S. Gubser, J. Maldacena, H. Ooguri, and Y. Oz, Phys. Rep. **323**, 183 (2000).
[4] G. T. Horowitz and V. E. Hubeny, Phys. Rev. D **62**, 024027 (2000).
[5] V. Cardoso and J. P. S. Lemos, Phys. Rev. D **64**, 084017 (2001).
[6] I. G. Moss and J. P. Norman, Classical Quantum Gravity **19**, 2323 (2002).
[7] B. Wang, C. Lin, and E. Abdalla, Phys. Lett. B **481**, 79 (2000).
[8] V. Ferrari and L. Gualtrier, arXiv:gr-qc/0709.0657.
[9] S. Hod and T. Pirani, Phys. Rev. D **58**, 024017 (1998).
[10] S. Hod and T. Pirani, Phys. Rev. D **58**, 024018 (1998).
[11] S. Hod and T. Pirani, Phys. Rev. D **58**, 024019 (1998).
[12] R. A. Konoplya, Phys. Lett. B **550**, 117 (2002).
[13] R. A. Konoplya and A. Zhidenko, Phys. Rev. D **76**, 084018 (2007).

[14] R. A. Konoplya, Phys. Rev. D **66**, 084007 (2002).
[15] R. Aros, C. Martinez, R. Troncoso, and J. Zanelli, Phys. Rev. D **67**, 044014 (2003).
[16] D. Birmingham and S. Mokhtari, Phys. Rev. D **74**, 084026 (2006).
[17] A. Lopez-Ortega, Gen. Relativ. Gravit. **39**, 1011 (2007).
[18] A. Lopez-Ortega, Gen. Relativ. Gravit. **38**, 1565 (2006).
[19] M. Bañados, C. Teitelboim, and J. Zanelli, Phys. Rev. Lett. **69**, 1849 (1992); M. Bañados, M. Henneaux, C. Teitelboim, and J. Zanelli, Phys. Rev. D **48**, 1506 (1993).
[20] D. Birmingham, Phys. Rev. D **64**, 064024 (2001).
[21] D. Birmingham, I. Sachs, and S. N. Solodukhin, Phys. Rev. Lett. **88**, 151301 (2002).
[22] V. Cardoso and J. P. S. Lemos, Phys. Rev. D **63**, 124015 (2001).
[23] E. Abdalla, B. Wang, A. Lima-Santos, and W. G. Qiu, Phys. Lett. B **538**, 435 (2002).
[24] S. Fernando, Gen. Relativ. Gravit. **36**, 71 (2004).
[25] A. Lopez-Ortega, Gen. Relativ. Gravit. **37**, 167 (2005).
[26] K. C. K. Chan, Phys. Lett. B **373**, 296 (1996).
[27] E. W. Hirshmann and D. L. Welch, Phys. Rev. D **53**, 5579 (1996).
[28] M. Kamata and T. Koikawa, Phys. Lett. B **353**, 196 (1995).
[29] G. Clement, Phys. Lett. B **367**, 70 (1996).
[30] S. Fernando and F. Mansouri, Commun. Math. Theor. Phys. **1**, 14 (1998).
[31] K. C. K. Chan and R. B. Mann, Phys. Rev. D **50**, 6385 (1994).
[32] G. Horowitz, arXiv:hep-th/9210119.
[33] M. Abramowitz and A. Stegun, *Handbook of Mathematical Functions* (Dover, New York, 1977)
[34] S. Fernando, Gen. Relativ. Gravit. **37**, 461 (2005).
[35] D. N. Page, Phys. Rev. D **16**, 2402 (1977).
[36] S. S. Gubser and I. R. Klebanov, Nucl. Phys. **B482**, 173 (1996).
[37] M. Setare, Classical Quantum Gravity **21**, 1453 (2004).
[38] M. Setare, Phys. Rev. D **69**, 044016 (2004).
[39] G. W. Gibbons and C. M. Hull, Phys. Lett. **109B**, 190 (1982).
[40] H. Onozawa, T. Okumura, T. Mishima, and H. Ishihara, Phys. Rev. D **55**, R4529 (1997).